

Attractive and repulsive functions of Slit are mediated by different receptors in the *Drosophila* trachea

Camilla Englund¹, Pär Steneberg¹, Lyudmila Falileeva¹, Nikos Xylourgidis² and Christos Samakovlis^{1,2,*}

¹Umeå Centre for Molecular Pathogenesis, Umeå University, S-901 87 Umeå, Sweden

²Department of Developmental Biology, Wenner-Gren Institute, Stockholm University, S-106 91 Stockholm, Sweden

*Author for correspondence (e-mail: christos@devbio.su.se)

Accepted 5 August 2002

SUMMARY

Oxygen delivery in many animals is enabled by the formation of unicellular capillary tubes that penetrate target tissues to facilitate gas exchange. We show that the tortuous outgrowth of tracheal unicellular branches towards their target tissues is controlled by complex local interactions with target cells. Slit, a phylogenetically conserved axonal guidance signal, is expressed in several tracheal targets and is required both for attraction and repulsion of tracheal branches. Robo and Robo2 are expressed in different branches, and are both necessary for the correct orientation of branch outgrowth. At the CNS

midline, Slit functions as a repellent for tracheal branches and this function is mediated primarily by Robo. Robo2 is necessary for the tracheal response to the attractive Slit signal and its function is antagonized by Robo. We propose that the attractive and repulsive tracheal responses to Slit are mediated by different combinations of Robo and Robo2 receptors on the cell surface.

Key words: Tracheal branching, Cell migration, Robo, Slit, *Drosophila*

INTRODUCTION

Directed cell migration is essential in the development of many organs. Most of the known cell navigation signals have been identified from studies of migrating neurons responding to attractive or repulsive cues provided by surrounding glial or neuronal cells. In this study, we show that neurons and glia also steer the complex pathfinding of tracheal cells in the central nervous system (CNS) of *Drosophila*.

The tracheal system develops from 20 clusters of ectodermal cells, each containing about 80 cells. After invagination and without further cell division, each epithelial cluster extends sequentially primary, secondary, fusion and terminal branches to generate the tubular network that facilitates larval respiration (Manning and Krasnow, 1993; Samakovlis et al., 1996a). The regular outgrowth pattern of the primary branches is determined by the localized expression of signaling factors in the surrounding tissues. Among these signals, Branchless (Bnl), a member of the Fibroblast Growth Factor family, first directs the outgrowth of multicellular branches to its site of expression, and it then induces the activation of a set of terminal branching genes in the leading cells of the primary branches (Sutherland et al., 1996). Single terminal cells then form a unicellular branch, migrate over substantial distances and finally stretch and bind to distinct parts of the target tissue to facilitate respiration. A single terminal cell of each ganglionic branch (GB), for example, targets each hemisegment of the embryonic ventral nerve cord (VNC). A cluster of *bnl*-expressing cells just outside the CNS attracts the GB

toward the CNS. The GB cells migrate ventrally along the intersegmental nerve (ISN), but just before reaching the entry point into the CNS, they break their contact with ISN and turn posteriorly to associate with the segmental nerve (SN) (Englund et al., 1999). This substrate switch is promoted by the expression of *adrift* (*aft*), a *bnl*-induced gene required in the trachea for efficient entry into the CNS (Englund et al., 1999). Inside the CNS, the GB1 cell extends over a distance of about 50 µm, from the entry point into the CNS via four different neural and glial substrata to its target on the dorsal side of the neuropil (Englund et al., 1999). During the first 20 µm of its journey inside the CNS, the GB1 cell moves its cell body and nucleus along the exit glia, the SN and ventral longitudinal glia towards the midline (Englund et al., 1999) (Fig. 1A). The rest of the path is covered by a long cytoplasmic projection that turns dorsally at the midline and reaches the dorsal part of the neuropil by the end of embryogenesis (Fig. 1B,C). The signals that guide GB1 migration inside the CNS are not known but the substrata that the GB contact along its path could potentially provide important guidance cues.

We investigate the importance of glial substrata in guiding the GB1 inside the CNS. By genetic ablation experiments, we show that different glial cells provide distinct positional cues to the trachea. Longitudinal glia are first required for GB1 migration towards the midline, whereas midline and channel glia are necessary for inhibiting it from crossing the midline and to make it migrate dorsally through the neuropil. We show that Slit signaling plays a major role in the migration of the GB1 cell. Slit is produced by midline cells (Rothberg et al.,

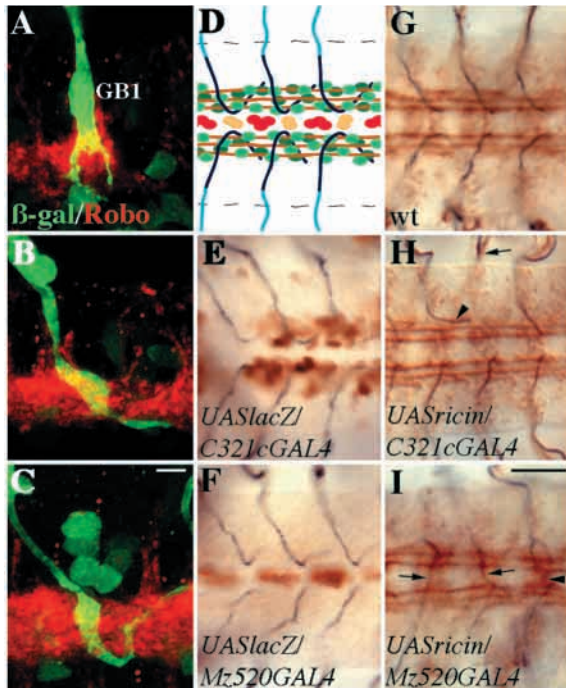


Fig. 1. Ablations of glial cells affect tracheal cell guidance. (A-C) Confocal projections showing the morphology of the ganglionic branch tip cell (GB1) visualized in green by the *1-eve-1 lacZ* cytoplasmic marker. Robo staining, in red, was used to mark the longitudinal connectives. (A) At stage 15, GB1 has reached the ventral side of the neuropil and has extended several cytoplasmic processes. (B) At stage 16, GB1 turns at the CNS midline and extends one cytoplasmic protrusion dorsally and posteriorly along the dorsoventral channel glia to reach the dorsal side of the neuropil. The GB1 nucleus has reached its position just ventral of the longitudinal connective. (C) By late stage 16, GB1 has extended laterally and posteriorly on the dorsal side of the neuropil. (D) Schematic drawing showing a ventral view of three pairs of GBs and their path in the wild-type embryonic stage 16 nerve cord. Inside the CNS, GB1 (dark blue) contacts first the ventral longitudinal glia (pale green). It turns before reaching the ventral midline and the midline glia (red), and migrates dorsally at the midline in close contact with channel glia (yellow). When GB1 reaches the dorsal side of the neuropil, it associates with the dorsal longitudinal glia (dark green) and extends laterally and posteriorly. The stalk cell of the ganglionic branch, GB2 is shown in pale blue, longitudinal axon tracts in brown and the borders of the CNS with broken lines. (E-I) GBs are misrouted when longitudinal glia are ablated by the expression of *UAS-ricinA*. The tracheal lumen of stage 16 embryos is shown in blue and the longitudinal and midline glia cells in E,F or the longitudinal connectives in G-I in brown. (E) Longitudinal and (F) midline glial cells are shown by the expression of *UAS-lacZ* driven by *C321c-GAL4* and by *Mz520-GAL4*, respectively. (H) When longitudinal glia are ablated GBs stall outside CNS (arrow) or turn to migrate posteriorly before crossing the longitudinal tracts (arrowhead). Ablation of midline glial cells leads to midline crosses (I) of the GBs (arrows) and the longitudinal axon tracts (arrowhead) (compare with G). All panels show ventral views, anterior is towards the left. Scale bars: 4 μ m in A-C; 8 μ m in E-I.

1988; Rothberg et al., 1990) and prevent GBs from crossing the midline of the VNC. Slit is also required as an attractant for the outgrowth of the primary, dorsal and visceral branches. The Slit receptors Roundabout (Robo) (Brose et al., 1999; Kidd

et al., 1998a) and Roundabout 2 (Robo2) (Rajagopalan et al., 2000a; Simpson et al., 2000a) are both required in the trachea independently of their function in axonal migration. The analysis of the tracheal *robo* and *robo2* mutant phenotypes suggests that they may mediate different responses to the Slit signal. These results provide a first insight into the signaling mechanisms that guide the GB in the CNS, and identify an in vivo system for the study of bi-functional role of Slit in epithelial cell guidance at the level of single cells.

MATERIALS AND METHODS

Fly stocks

The following null or strong loss-of-function alleles were used: *slit/CyOactlacZ* (Rothberg et al., 1990), *robo²⁵⁷⁰/CyOactlacZ* (Kidd et al., 1998a), *bprpknrobo/CyOwglacZ* (all provided by C. Goodman), *robo2^{1,4,8}/CyOwglacZ*, *robo^{GA285}robo2⁵/CyOwglacZ* (all provided by B. Dickson) (Rajagopalan et al., 2000a), and *comm⁰⁷²/TM3ubxlacZ* and *comm^{B204}/TM3ubxlacZ* (both provided by C. Klämbt) (Hummel et al., 1999).

The following GAL4 and UAS strains were used: *w;C321c* (on second chromosome, provided by A. Hidalgo) (Hidalgo et al., 1995); *Mz520* and *Mz820* (on second chromosome, both provided by G. Technau) (Ito et al., 1995); *SRF-GAL4* (on third chromosome, K. Guillemin, personal communication); *btl-GAL4* (Shiga et al., 1996); *elav-GAL4* (#458); *twi-GAL4* (#914) and *en-GAL4* (#233) (all three from Bloomington Stock Center); *UAS-lacZ* (Brand and Perrimon, 1993); *w;UAS-ricinA/CyOwgen¹¹lacZ* (Hidalgo et al., 1995); *UAS-robo* (Kidd et al., 1998a), *UAS-slit* (Kidd et al., 1999) and *UAS-comm* (Kidd et al., 1998b) (all three provided by C. Goodman); *UAS-robo* and *UAS-robo2* (HA-tagged, both provided by B. Dickson) (Rajagopalan et al., 2000b); and *UAS-EGFPF/CyO*, which harbors an enhanced GFP construct that is targeted to the cellular membrane (provided by R. Palmer) (Finley et al., 1998).

The enhancer trap marker *1-eve-1* (Tracheal 1), which was used to visualize tracheal cells, has been described previously (Perrimon et al., 1991).

Immunostaining

Embryo fixation, staining, light and confocal fluorescence microscopy were as described (Samakovlis et al., 1996b). The tracheal lumen-specific antibody used was mAb2A12 (Developmental Studies Hybridoma Bank, University of Iowa) diluted 1:3. The anti-DSRF monoclonal antibody was mAb2-161 (1:2000) from M. Gilman (Ariad Corporation, Boston, MA). Rabbit antiserum against β -galactosidase (Cappel) was used at 1:1500. Rabbit antiserum against Robo2 (from B. Dickson) (Rajagopalan et al., 2000a) was used at 1:100 for immunofluorescence. The mouse monoclonal antibodies against Robo (mAb13C9) (Kidd et al., 1998a) and Fasciclin II (mAb1D4) (Van Vactor et al., 1993) were used at 1:10 and 1:50, respectively (both from C. Goodman). Mouse monoclonal against Slit (C555.6d) was diluted 1:10 (from B. Dickson) (Rothberg et al., 1990). Rabbit antiserum against GFP (Molecular Probes) was diluted 1:1000. Anti-HA mAb16B12 (Berkeley Antibody Company) was used at 1:1000 or 1:400. Biotin-, Cy2- and Cy3-conjugated (Jackson Laboratories) and Alexa Fluor-568- and -488-conjugated (Molecular Probes) secondary antibodies were used at 1:300, 1:500 and 1:400, respectively. Embryo staging was according to Campos-Ortega and Hartenstein (Campos-Ortega and Hartenstein, 1985).

Ablations, rescue and gain-of-function experiments

The ablation, rescue and gain-of-function experiments were carried out using the UAS-GAL4 system (Brand and Perrimon, 1993). For all the UAS-GAL4 crosses mentioned below, embryos were collected for

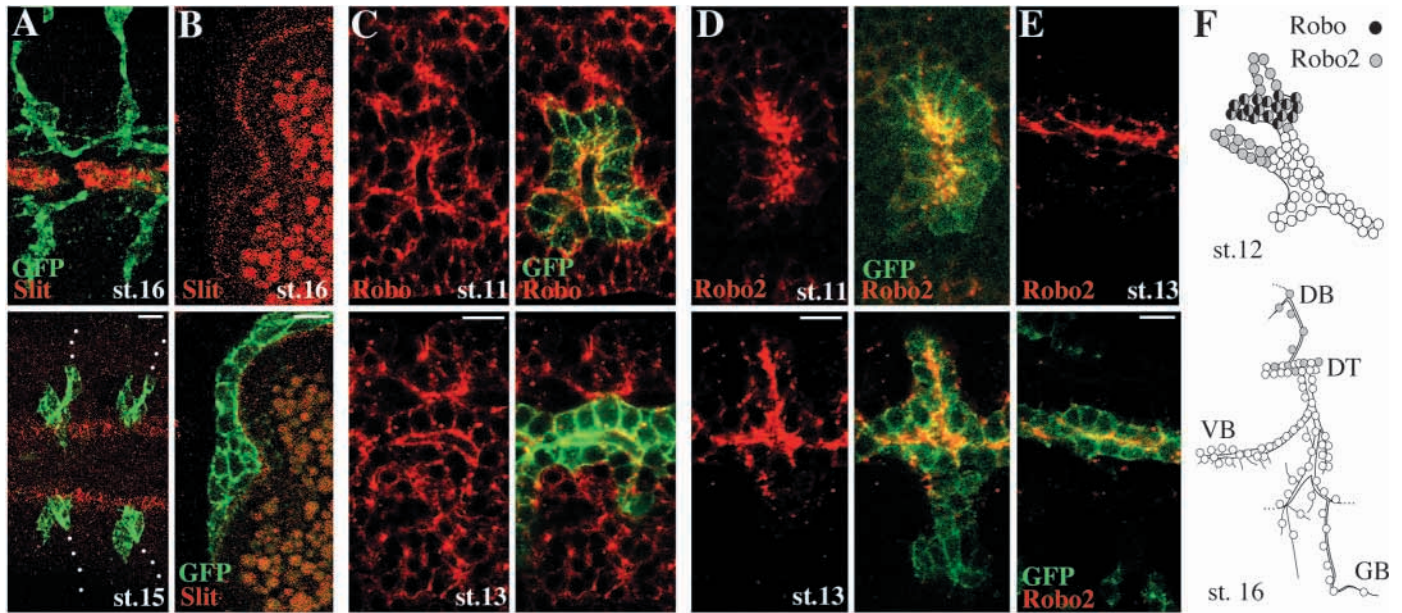


Fig. 2. Expression of Slit and its receptors during tracheal development. Confocal analysis of wild-type embryos carrying the UAS-EGFPF marker expressed under the control of the tracheal-specific driver *btl-GAL4*, double stained with anti-GFP to visualize the tracheal cells in green and anti-Slit (A,B), anti-Robo (C) or anti-Robo2 (D,E) in red. (A) Slit expression at the ventral midline close to the migrating tracheal tip cells of the ganglionic branch (top) and at the dorsal side, in cells just underneath the migrating dorsal branches (bottom, dorsal view). Dotted lines indicate the part of the tracheal dorsal branches that is out of focus. (B) Slit expression at the contacts of the gut epithelium and the tracheal visceral branches (anterior is upwards). (C-E) Lateral views showing the expression of Robo and Robo2 in the invaginating tracheal cells at stage 11 (C,D, top), the dorsal trunk and dorsal branch at stage 13 (C,D, bottom). (E) Robo2 expression in the growing visceral branches. (F) Summary drawings of Robo and Robo2 expression in different branches (DB, dorsal branch; DT, dorsal trunk; VB, visceral branch; GB, ganglionic branch) at stages 12 and 16. At stage 12 (top) both Robo (black) and Robo2 (gray) are expressed in cells of the DT, but Robo2 is also expressed in the DB and the VB. After stage 13, Robo is no longer detectable in the trachea, whereas Robo2 is expressed in DT and DB until the end of embryogenesis (bottom). Scale bars: 8 μ m in A-E.

6 hours at 20°C and then transferred to 29°C for 10 hours to maximize GAL4 activity and they were analyzed with markers accordingly.

To ablate glial cells *w;UAS-ricinA/CyOwg^{en11}lacZ* flies were crossed to *C321c* driver line, which expresses GAL4 in longitudinal glia, or to *Mz520* and *Mz820*, express GAL4 in midline glia and channel glia in the CNS, respectively. Embryos were stained with mAb2A12, anti- β -galactosidase and mAb1D4 (which stains Fasciclin II-positive axons in the longitudinal connectives). To rescue the tracheal phenotypes of *robo^{z570}* and *robo2^{1,4,8}* mutants, we used the *SRF-GAL4* driver, which expresses GAL4 in all tracheal terminal cells from stage 13, to drive expression of *UAS-robo* and *UAS-robo2*. In addition, the reciprocal tracheal rescue and the *UAS-robo* and *UAS-robo2* tracheal gain-of-function experiments were made using these strains and embryos were analyzed with mAb2A12, mAb2-161 (marks tracheal terminal cells), mAb1D4, mAb16B12 and mAb13C9. To rescue the *robo* mutant CNS phenotype *UAS-robo* was driven by *elav-GAL4*, which is expressed in all postmitotic neurons in the CNS. For the *comm* gain-of-function experiment, we used the *UAS-comm* and the *btl-GAL4* driver, which expresses GAL4 in all tracheal cells from stage 11. For the *slit* gain-of-function experiment in the CNS, we used *C321c-GAL4* and *elav-GAL4* strains to drive expression of *UAS-slit*, and to misexpress *UAS-slit* in the gut epithelium and in the epidermis, we used the *twi-GAL4* and *en-GAL4* drivers, respectively.

RESULTS

Ablation of glia affects ganglionic branch pathfinding

We analyzed the GB1 cell extensions and migration inside the

CNS in embryos carrying the *1-eve-1 lacZ* marker, an enhancer trap insertion into the *trachealess (trh)* gene, which is expressed in all tracheal cells from stage 11 (Perrimon et al., 1991), with antibodies against β -galactosidase and Robo, a marker for the longitudinal axons. At stage 15 GB1 enters the CNS and migrates ventrally, extending broad cytoplasmic protrusions in different directions (Fig. 1A). These protrusions contact the ventral longitudinal glia on the ventral side of the nerve cord. At early stage 16, the GB1 cell comes close to the midline but there it turns dorsally and posteriorly (Fig. 1B). By late stage 16, GB1 has sent a long projection through the channel glial cells to reach the longitudinal glia at the dorsal side of the neuropil (Fig. 1C) (Englund et al., 1999). The stereotyped route of GB1 and its contact with different glial cells suggested that its path may be dictated by its contacts or signals from its substrates. We used the UAS-GAL4 system (Brand and Perrimon, 1993) with glial specific GAL4 drivers to express *lacZ* or the toxin Ricin A gene (Hidalgo et al., 1995; Moffat et al., 1992) in specific subsets of glial cells. The effect of glial ablations on GB1 and axonal migration was analyzed using a tracheal lumen-specific antibody, and the mAb1D4 (anti-Fasciclin II) (Van Vactor et al., 1993) that stains the major longitudinal axon tracts. The expression of the *lacZ* marker driven by the GAL4 strains used in these experiments was mosaic: not all of the targeted glial cells in each neuronal hemisegment expressed the marker (Fig. 1E,F). Consequently, the expression of Ricin A and the ablations was also mosaic.

When we ablated longitudinal glia with the *C321c-GAL4*

line (Hidalgo et al., 1995), 31% of GBs ($n=112$) stalled or turned to migrate posteriorly before reaching the longitudinal connectives (Fig. 1H and data not shown). The formation of longitudinal axon tracts as revealed by mAb1D4 staining was not detectably affected in these embryos, suggesting that longitudinal glia might have a function in guiding the GB to the ventral side of the neuropil and across the longitudinal tracts. Ablation of midline glia using the *Mz520-GAL4* line (Ito et al., 1995) caused a different phenotype. Nine percent of the GBs ($n=112$) crossed the midline, and 5% lingered along the midline or turned anteriorly (Fig. 1I). Staining with mAb1D4 showed that some axons of the longitudinal tracts also were crossing the midline (Fig. 1I). These results suggest that midline glia influence GB1 turning either through direct signaling or indirectly by affecting the structure of surrounding axon trajectories. We have also expressed Ricin A in subperineurial and channel glia using the *Mz820-GAL4* line (Ito et al., 1995). In these embryos, 6% of GBs ($n=126$) turned to migrate posteriorly before crossing the longitudinal connectives and 8% lingered around the midline (data not shown). We did not observe any defects in the Fasciclin II-positive axons, suggesting that dorsoventral channel glia may provide an instructive landmark for the extension of GB1 from the ventral to the dorsal side of the neuropil.

In summary, the above results suggest that the different types of glia that become contacted by GB1 inside the VNC provide distinct guidance landmarks for its migration. As the ablation of longitudinal glia results in stalls or misroutings before the longitudinal tracts, these cells are likely to have an attractive function for GB1. The ablation of midline and channel glia leads to midline crossings and lingering, suggesting that these cells may provide both direct or indirect attractive and repulsive landmarks.

Expression of Slit and its receptors during tracheal development

A major determinant of axonal pathways inside the CNS is the repellent signal Slit. Midline cells express Slit, a large extracellular matrix protein (Rothberg et al., 1988; Rothberg et al., 1990) that functions both as a short- and long-range repellent, controlling axon crossing at the midline and mesodermal cell migration away from the midline (Battye et al., 1999; Kidd et al., 1999). In axon guidance, the Slit repulsive signal is mediated by the Roundabout (Robo) receptors (Brose et al., 1999; Kidd et al., 1999; Kidd et al., 1998b; Rajagopalan et al., 2000a; Simpson et al., 2000a). Different axons express different combinations of the three receptors, which determine the distance of their projections from the midline along the longitudinal fascicles (Rajagopalan et al., 2000b; Simpson et al., 2000b). The midline crossing phenotypes of GBs in embryos expressing Ricin A in the midline glia suggests that Slit signaling may also guide GB1 in its turn away from the midline. We double stained embryos expressing GFP under the control of the pan-tracheal *btl-GAL4* driver (Shiga et al., 1996), which drives expression of GAL4 in all tracheal cells from stage 11, with antibodies against GFP and Slit or its receptors, and analyzed their expression by confocal microscopy. The GB1 cell comes close to the midline source of Slit at early stage 16 but it then turns dorsally and posteriorly at the midline (Fig. 2A, top). Slit is also expressed in several other tissues close to the migrating tracheal branches.

At early stage 14 in the dorsal side of the embryo, two rows of migrating mesodermal cells that will form the larval heart express Slit. These cardioblasts are in close proximity to the two leading cells of the tracheal dorsal branches (DBs), which also migrate towards the dorsal midline and give rise to the dorsal anastomosis (DB2) and the dorsal terminal branch (DB1) (Fig. 2A, bottom). Slit expression is also detected from stage 13 on the surface of the midgut, at the sites of contact of the growing tracheal visceral branches (VBs) (Fig. 2B). Finally we detected Slit in lateral stripes of epidermal cells adjacent to the growing dorsal trunk (DT) and dorsal branches from stage 13 (data not shown). Are then the Slit receptors expressed in the trachea? Robo staining can be detected in all tracheal cells as they invaginate from the epidermis already at stage 11 (Fig. 2C, top). Its tracheal expression is decreased by stage 13, when it is only weakly expressed in the dorsal trunk (Fig. 2C, bottom). We were not able to detect any convincing expression of Robo in the trachea after stage 14, even when we analyzed serial optical sections of the GB1 cell along its path in the CNS (Fig. 1 and data not shown). Robo2 is also expressed in all tracheal cells from stage 11 (Fig. 2D, top) and it then becomes restricted to the dorsal trunk and dorsal and visceral branches by stage 13 (Fig. 2D, bottom; Fig. 2E) (Rajagopalan et al., 2000a). In contrast to Robo, which becomes undetectable in the trachea by stage 14, Robo2 expression is stronger and is maintained as late as at stage 16 in the DB1 and DB2 cells at the dorsal midline (data not shown). Robo3 expression could not be detected in the trachea (Rajagopalan et al., 2000a). The expression of Slit in tissues surrounding the developing trachea and the dynamic expression of its two receptors in different tracheal branches suggested a role for Slit signaling in tracheal branch outgrowth towards their target tissues.

Slit signaling is required for ganglionic branch turning at the midline

Although we could not detect the expression of any of the known Slit receptors in the GBs, the abrupt turn of GB1 when it comes close to the midline and the results from the midline cell ablation experiments prompted us to examine the potential role of Slit in the GB1 pathfinding. We first analyzed, *robo*, *robo2* and *slit* mutant embryos double stained with antibodies against the tracheal lumen and a tracheal nuclear marker. We also studied embryos of these genotypes, double stained for the tracheal lumen and Fasciclin II to correlate the tracheal and axonal phenotypes in the same embryos. In *robo* mutants, all GBs migrated into the VNC and the position of GB1 nucleus was not significantly affected (Fig. 3B). At the midline, 29% of GBs ($n=140$) crossed and 26% migrated unusually close to the midline, where they stalled or turned to migrate dorsally (Fig. 3B). The characteristic structure of the three longitudinal connectives in the same embryos was also severely disrupted by loops of axons crossing the midline several times (Kidd et al., 1998a) (Fig. 3G). In contrast to axons, GB1 crossed the midline only once and migrated along the longitudinal tracts of the contralateral hemisegment. This phenotype suggested that GB1 might not just passively follow the misrouted axons and argued that Robo might function as a repellent receptor in GB1 independently of its role in the neurons. It also suggests that *robo* is only required to prevent GB1 from crossing the midline and not to repel it once it has entered. If the GB1 phenotype in *robo* mutants is a primary effect caused by loss

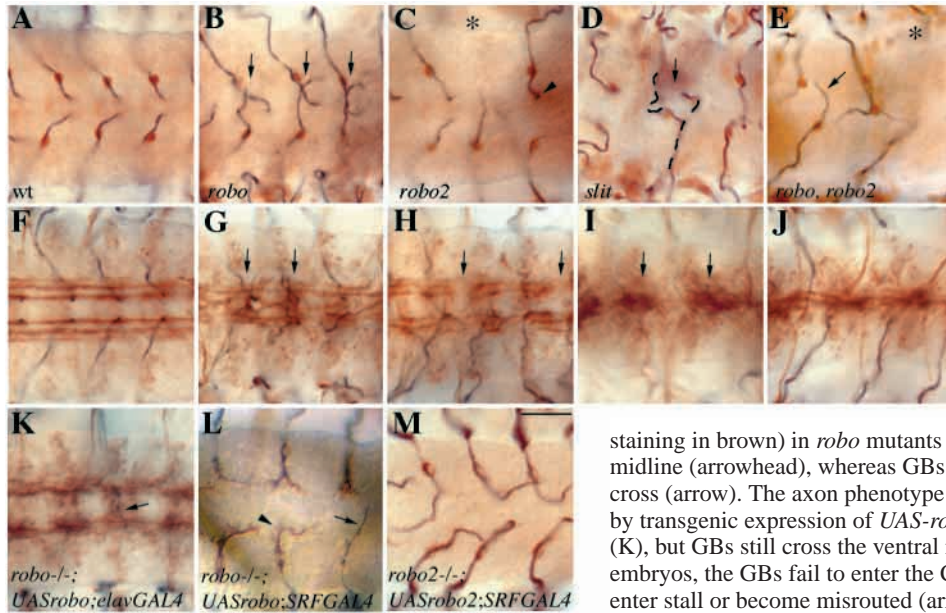


Fig. 3. Slit signaling is required for ganglionic branch turning at the midline. (A-M) Stage 16 embryos stained for the tracheal lumen in blue and the GB1 cell marker DSRF (A-E) or longitudinal connectives (F-K) in brown. In wild-type embryos (A), GBs turn posteriorly at the ventral midline but in *robo* and *slit* mutants (arrows in B and D) they cross it. The fascicles of the longitudinal connectives are separated in wild type (F), but cross the midline in *robo* mutants (arrows in G); in *slit* mutants (I), the fascicles are fused at the midline (arrows). (L) Transgenic tracheal expression of *UAS-robo* (anti-Robo

staining in brown) in *robo* mutants rescues GBs from crossing the ventral midline (arrowhead), whereas GBs with no detectable Robo expression still cross (arrow). The axon phenotype in *robo* mutant embryos is partially rescued by transgenic expression of *UAS-robo* in all neurons with the *elav-GAL4* driver (K), but GBs still cross the ventral midline (arrow in K). (C) In *robo2* mutant embryos, the GBs fail to enter the CNS (asterisk) and several of the GBs that do enter stall or become misrouted (arrowhead). (H) The longitudinal axon tracts are disrupted (arrows) and the outer fascicles fuse with the medial fascicles in *robo2* mutants. (M) The GB failure to enter the CNS in *robo2* mutants can be rescued by transgenic tracheal expression of *UAS-robo2* with the *SRF-GAL4* driver. (E) GBs in the double mutant *robo, robo2* fail to enter the CNS (asterisk) and cross the ventral midline (arrow) and the longitudinal axons collapse along the midline (J). These phenotypes are very similar to the phenotypes of *slit* mutants (D,I). Scale bar: 20 μ m in A-M.

of Robo in the trachea, it should be possible to rescue this phenotype by selectively expressing *robo* in GB1. We crossed an *UAS-robo* transgene and a *SRF-GAL4* driver construct, which expresses GAL4 in all tracheal terminal cells, into the *robo* mutant strain. The anti-Robo antibody was used to detect Robo protein deriving from the transgene. When Robo was expressed in the GB1 of *robo* mutants (*robo/robo;UAS-robo/SRF-GAL4*), none of the GBs crossed the midline (Table 1; Fig. 3L). Instead, 91% of the GBs that expressed Robo in GB1 ($n=118$) turned to migrate posteriorly prematurely (Fig. 3L). In these tracheal rescued *robo* mutants, 12% of the GB1 cells did not express any detectable Robo and 18% of these cells crossed the midline (Fig. 3L). Thus, Robo expression in the GB1 cells of *robo* mutants fully rescues the tracheal crossing of the midline phenotype. In the reciprocal experiment, where expression of *UAS-robo* in homozygous *robo* mutant embryos was driven in all neurons by the *elav-GAL4* strain (*elav-GAL4/+;robo/robo;UAS-robo/+*), the crossing of Fasciclin II-positive axons was significantly rescued (Kidd et al., 1998a) (Fig. 3K), but 21% of the GBs ($n=168$) still crossed the midline (Table 1; Fig. 3K). We conclude, that Robo is required in the GB1 tracheal cell to prevent it from crossing the CNS midline.

Robo2 acts as a long distance Slit receptor in the axons of the lateral longitudinal fascicles (Rajagopalan et al., 2000a; Simpson et al., 2000a). In *robo2* mutants, the more distant lateral fascicle is disrupted and its axons come closer to the midline and occasionally cross it (Rajagopalan et al., 2000a; Simpson et al., 2000a) (Fig. 3H). The analysis of the tracheal phenotypes of two *robo2* mutant alleles, *robo2⁴* and *robo2⁸*, produced similar results and revealed that the GB defects of *robo* and *robo2* mutants were different. Only 6% ($n=160$) of the branches crossed the midline in *robo2⁴* embryos and, in

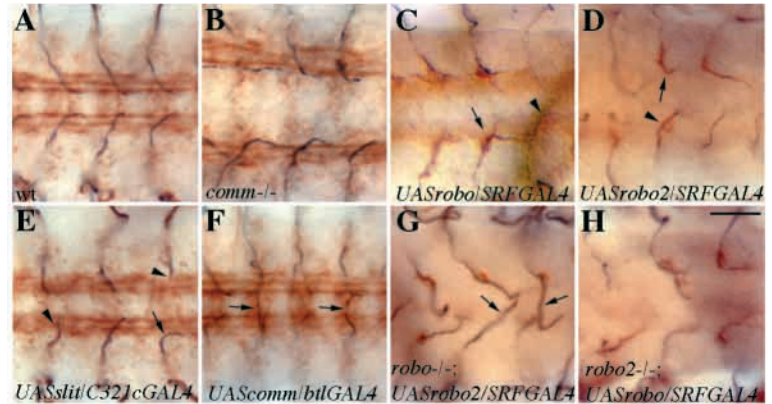
contrast to the *robo* mutant phenotype, these branches did not extend to the contralateral longitudinal connectives, they lingered around the midline instead. The most striking defect of *robo2* mutants was that 46% of the branches were stalled before reaching the midline turning point, and an additional 11% of them did not even enter the CNS (Fig. 3C) suggesting that *robo2* may be required earlier than *robo* for the migration of the GB1 cell towards the midline glia. We expressed a HA-tagged version of Robo2 in the GB1 cell under the control of the *SRF-GAL4* driver in *robo2⁴* embryos to assess whether we could rescue the mutant phenotypes. The embryos were double stained with antibodies against the tracheal lumen and HA to identify branches expressing *Robo2*. The number of GBs stalled outside the CNS was markedly reduced in these embryos (Fig. 3M), 1% ($n=220$) compared with 11% ($n=160$) in *robo2⁴* mutants, suggesting that *robo2* is required in the GB1 for its entry into the CNS. In the same experiment we did not observe any reduction of the number of branches that cross the midline, suggesting that this phenotype may be indirect or that the expression levels of transgenic Robo2 protein in the *robo2* mutants were not optimal for rescuing this phenotype. In fact,

Table 1. Rescue of *robo* tracheal phenotype by expression of an *UAS-robo* transgene

Genotype	Affected ganglionic branches* (%)
Wild type	0 ($n=280$)
<i>robo/robo</i>	29 ($n=140$)
<i>robo/robo;UAS-robo/SRF-GAL4</i>	0 ($n=118$)
<i>elav-GAL4/+;robo/robo;UAS-robo/+</i>	21 ($n=168$)

*Ganglionic branches that cross the midline.

Fig. 4. Overactivation of the Slit signaling pathway in the CNS can repel the ganglionic branches. (A–H) Stage 16 embryos stained to visualize the tracheal lumen in blue and the longitudinal axons (in A, B, E, F) in brown. (B) In *comm* mutants, GBs turn to migrate posteriorly before they reach the midline but after crossing the longitudinal tracts. The longitudinal axon tracts are further apart presumably due to the absence of commissures. (C) Ectopic expression of Robo in the GB1 cell (Robo staining in brown) using the *SRF-GAL4* driver results in GBs turning posteriorly before they cross the longitudinal tracts (arrow). GBs that do not overexpress Robo migrate closer to the midline before turning posteriorly (arrowhead). (D) Early turning of GB1 before the longitudinal axons (arrow) can also be seen in embryos with ectopic expression of *robo2* (embryos stained for a HA-tagged Robo2 in brown). Several of the Robo2 overexpressing GBs still reach the midline (arrowhead) in contrast to all the GBs that turn prematurely when they overexpress Robo in C. (E) Ectopic expression of Slit in the longitudinal glia using the *C321c-GAL4* driver leads to premature turning (arrow) and stalling (arrowheads) of GBs. (F) Several GBs cross the ventral midline (arrows) in response to general tracheal misexpression of *comm* using the *btl-GAL4* driver. (G) *UAS-robo2* overexpression in GB1 using the *SRF-GAL4* driver cannot rescue the GB midline crossing phenotype in *robo* mutants (arrows, embryos stained for HA-tagged Robo2 and the tracheal lumen). *UAS-robo* overexpression with the same driver can rescue the GB CNS entry phenotype in *robo2* mutants (H; embryos stained for Robo-HA and tracheal lumen). Scale bar: 20 μ m in A–H.



17% of the GB1s in these embryos turned prematurely before reaching the midline (Fig. 3M).

In *slit* mutants, the CNS axons enter the midline and remain there forming one large axon fascicle (Kidd et al., 1999; Rothberg et al., 1990) (Fig. 3I). When we looked at GB pathfinding in *slit* mutant embryos, we found defects both outside and inside the CNS. Practically all GBs were misrouted, and branches did not migrate in the same dorsoventral plane. We found that 17% of GBs ($n=154$) stalled outside or inside the CNS and that 37% crossed the midline (Fig. 3D). The tracheal phenotypes in *robo.robo2* double mutants were similar to the defects of *slit* embryos, 21% of the branches ($n=140$) stalled outside the CNS, 31% crossed the midline and 45% were misrouted (Fig. 3E).

This analysis indicates that Slit is an important regulator of GB1 pathfinding towards and inside the CNS. Slit function is mediated in the trachea by the Robo and Robo2 receptors. The differences in tracheal phenotypes in *robo* and *robo2* mutants, suggest that Robo2 functions as a long distance attractant receptor for Slit during GB1 migration towards the CNS, whereas Robo mediates the repellent function of Slit inside the CNS, at the ventral midline.

Ectopic activation of Slit signaling redirects GB1 away from the midline

To further dissect the function of Slit and its receptors in GB1 migration we studied the effects of over activation of the pathway by either driving *slit* expression in longitudinal glia or manipulating the expression levels of *robo* and *robo2*.

Ectopic expression of *slit* in the longitudinal glia (*C321c-GAL4/+;UAS-slit/+*) causes stalls and premature turns in 37% of the GBs (Fig. 4E) suggesting that elevated levels of *slit* are sufficient to inhibit and repel GB1 migration inside the CNS. The longitudinal tracts in these embryos are formed normally as judged by mAb1D4 staining (Fig. 4E).

Robo and Robo2 expression can be post-translationally downregulated by Commissureless (Comm), a transmembrane protein that is expressed on the CNS midline cells during the formation of axon commissures (Tear et al., 1996). Comm is

necessary to decrease Robo expression on commissural axons thereby allowing them to cross the midline (Kidd et al., 1998b; Seeger et al., 1993). In *comm* mutants, Robo fails to be downregulated, no axons cross the midline and as a result no commissures are formed (Fig. 4B). In *comm* mutants, 97% of GBs ($n=140$) stalled or turned to migrate dorsally and posteriorly prematurely, before reaching the midline (Fig. 4B), suggesting that Comm is also modulating the levels of Robo in the trachea. We hypothesized that if Robo is downregulated by Comm, then transgenic expression of *comm* in the trachea might lead to downregulation of Robo in GB1 and a *comm* 'gain-of-function' phenotype where GB cross the midline. To test this, we crossed *UAS-comm* flies to the *btl-GAL4* line (Shiga et al., 1996). In these embryos (*UAS-comm/+;btl-GAL4/+*) the longitudinal axon tracts looked normal but 17% of the GBs ($n=168$) crossed the midline, 14% turned anteriorly at the midline and 15% stalled prematurely (Fig. 4F). These tracheal phenotypes are similar to the defects seen in *slit* mutant embryos and further argue for the role of Robo receptors in GB migration.

To overexpress *robo* and *robo2* in GB1 cells, we used the *SRF-GAL4* driver and epitope tagged forms of receptor transgenes, *UAS-roboHA* and *UAS-robo2HA*, which express similar levels of protein, as judged by immunohistochemical staining. These constructs were chosen to allow comparisons of the different phenotypes caused by the overexpression of the *robo* or *robo2* in the trachea. In *UAS-roboHA/SRF-GAL4* embryos, 55% of the HA-expressing GBs ($n=104$) turned prematurely to migrate posteriorly before coming close to the midline, and 16% stalled at the level of the longitudinal tracts (Fig. 4C). The premature turning phenotype resembles the tracheal defects in *comm* mutants and argues for a midline repulsive function for *robo* in GB1. The same phenotype was evident in embryos expressing an untagged version of *UAS-robo* under the control of the same driver, but there 94% of the Robo-expressing branches ($n=104$) were turning prematurely. In *UAS-robo2HA/SRF-GAL4* embryos, only 12% of the GBs expressing HA ($n=105$) turn to migrate posteriorly prematurely (Fig. 4D). The quantitative differences in the turning phenotype

of the overexpression experiments, taken together with the qualitative differences in the loss-of-function phenotypes for both receptors, suggest that *robo2* plays a minor role in GB1 pathfinding inside the CNS and that *robo* is the major repellent receptor at the midline.

Robo can rescue *robo2* but Robo2 can not rescue *robo* phenotypes

To further separate the potentially different functions of *robo* and *robo2*, we attempted to rescue the GB1 phenotype of one mutant by ectopically expressing a transgene encoding the tagged form of the other receptor. Overexpression of Robo in the GB1 cell of *robo2* mutants (detected by staining against HA) can partially rescue the entry into the CNS phenotype from 15% ($n=238$) in *robo2⁸/robo2⁴* embryos to 3.5% ($n=123$) in rescue embryos (*robo2⁴/robo2⁸; UAS-roboHA/SRF-GAL4*) (Fig. 4H). Overexpression could also rescue the weak midline crossing phenotype of *robo2*. None of the GBs crossed the midline compared with the 6% midline crossing phenotype in *robo2⁸/robo2⁴*. In addition, *robo* overexpression in *robo2* mutants caused a gain-of-function phenotype with 50% of the branches turning prematurely inside the CNS (Fig. 4H), similar to the *robo* overexpression phenotype in wild-type embryos. Thus, *robo* expression in the GB1 cells of *robo2* mutant rescues the CNS entry and midline crossing phenotypes. When Robo2 was ectopically expressed in GB1 of *robo* mutant embryos (*robo/robo;UAS-robo2HA/SRF-GAL4*), it did not provide substantial rescue activity. Twenty-two percent of GBs ($n=111$) still crossed the midline compared with 29% ($n=140$) in the *robo* mutant (Fig. 4G). In addition, *robo2* overexpression induced slightly fewer gain-of-function premature turns in *robo* mutants (7% compared with 11% in the wild type). These results argue that although *robo* misexpression can substitute for the absence of *robo2* during the migration of GB1 towards the CNS, overexpression of *robo2* can not significantly substitute for *robo* in its repellent function at the midline.

Functions of Slit and its receptors in other tracheal branches

The dynamic expression of Slit in several tracheal targets and the branch-restricted expression of *robo* and *robo2* during tracheal development suggested an additional role of Slit signaling in tracheal branches that do not target the CNS. We analyzed *slit*, *robo* and *robo2* embryos carrying the *1-eve-1 lacZ* marker, in order to visualize defects in tracheal cell migration and branching. In late stage 16 *slit* mutant embryos, the migration of the dorsal branches towards the heart was disrupted. Twenty percent of the branches ($n=100$) were either completely missing or stalled at various lengths (Fig. 5C). In addition, 28% of the branch fusion events that interconnect the tracheal network of either side of the embryo over the dorsal midline were also disrupted. Given the expression of Slit in the developing heart from stage 14, this phenotype suggests an attractive function for Slit in dorsal branch migration towards the dorsal midline of the embryo. *slit* embryos showed also defects in the migration of the GBs towards the lateral and ventral muscles and the CNS (Fig. 5F). In *slit* mutants, the cells of the ganglionic branches appeared to be extending projections towards the muscles but their directions were random and they were falling back towards the lateral trunk (Fig. 5F). Slit protein was also detected along the developing midgut at the attachment sites of the visceral

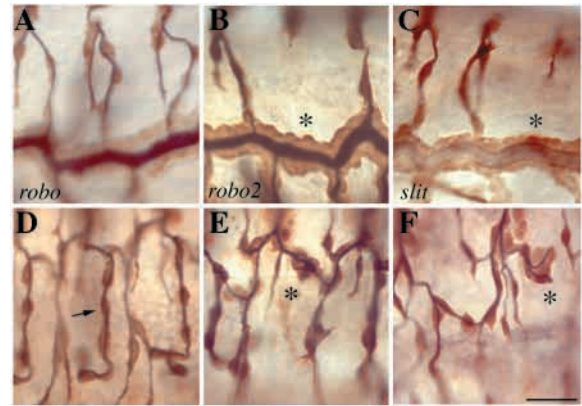


Fig. 5. Slit signaling is required for the outgrowth of tracheal branches outside the CNS. Lateral view of stage 16 embryos carrying one copy of the *1-eve-1 lacZ* marker stained to visualize tracheal cells and lumen. In *robo2* (B) and *slit* (C) mutant embryos outgrowth of the dorsal branches (DBs) is disrupted, resulting in missing (asterisks) or short DBs. In *robo* mutants (A), DB outgrowth is not affected. Several of the GBs in *robo2* (E) and *slit* (F) mutants are shorter and misrouted (asterisks). In *robo* mutants (D), GBs migrate ventrally as in wild-type embryos (arrow in D). Scale bar: 20 μ m in A-F.

branches (Fig. 2B). In *slit* mutants, all primary visceral branches grew towards the gut but the migration of the secondary branches on the target appeared irregular in some embryos with occasional projections extending more dorsally or ventrally along the midgut (data not shown). The tracheal phenotypes of *robo2⁸* mutants were similar to the defects of *slit* embryos. Eighteen percent of the dorsal branches ($n=220$) were stalled or missing in *robo2* embryos and 30% of the remaining branches that had extended towards the dorsal midline failed to fuse over the heart (Fig. 5B). In addition, as in *slit* embryos, the outgrowth of the GBs from the lateral trunk (Fig. 5E) was also sporadically affected. We could not detect any primary branch outgrowth phenotypes, in *robo* mutants (Fig. 5A,D). We have carefully examined more than 20 embryos from two different *robo* alleles and we conclude that *robo* is not required for the migration of tracheal branches towards targets outside the CNS. Every *slit* and *robo2* mutant embryo analyzed shows defects in the outgrowth of the dorsal branches and the extension of the fusion branches over the dorsal midline, the expression pattern and mutant phenotypes of *slit* and *robo2* mutants suggest that the expression of Slit outside the CNS provides an attractant signal for the tracheal cells and that the tracheal receptor for this signal is Robo2.

Ectopic Slit attracts tracheal branches to its sites of expression

If Slit is an attractive signal for the migration of the dorsal and visceral branches towards their targets, its ectopic expression in other tissues should attract tracheal branches towards the new expression sites. We expressed *UAS-slit* with the *en-GAL4* driver in stripes of epidermal cells along the dorsoventral axis located above the growth tracts of the dorsal branches (Fig. 6A). In these embryos, 23% of the dorsal trunk branches ($n=340$) that normally extend anteriorly and posteriorly to interconnect the ten tracheal metameres on either side of the

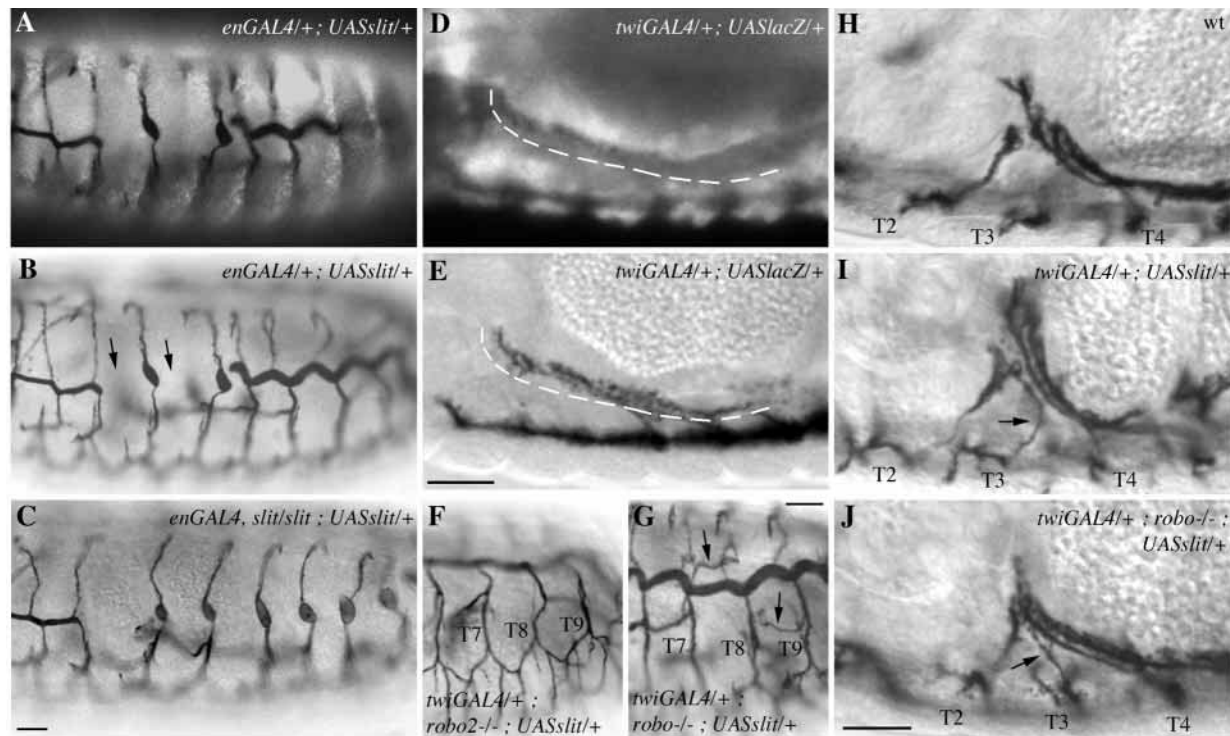


Fig. 6. Tracheal branches are attracted to sites of ectopic Slit expression. (A–J) Embryos stained to visualize the tracheal lumen and double stained for Slit (A,B) and β -galactosidase (D,E), to visualize the sites of ectopic Slit and β -gal expression. (A) Ectopic expression of Slit in epidermal stripes, induced using the *en-GAL4* driver, disrupts the anterior and posterior elongation of the dorsal trunk (DT) branches (arrows in B); the dorsal trunk appears to extend dorsoventrally along the *en-GAL4* stripes. (C) Removing endogenous Slit expression results in a stronger DT phenotype. (D) β -Gal expression driven by *twi-GAL4* shows that the driver directs UAS-transgene expression in the gut epithelia at stage 13, when the tracheal visceral branches (VBs) (E) start migrating towards and along the surface of the gut. The broken line indicates the terminal cells of the VB that are in close contact with the gut. (H) In wild-type embryos, the VBs from metamere T2 and T4 migrate towards the anterior part of the midgut. The T3 metamere does not form a VB. (I) Ectopic expression of *UAS-slit* with the *twi-GAL4* driver can induce formation of additional VBs from metamere T3 (arrow in I). In *robo* mutants, the ectopic expression of Slit results in formation of additional VBs from T3 and also from other metameres (arrows in J,G; dorsal and lateral views, respectively). The increased level of branch formation in response to ectopic Slit expression cannot be detected in *robo2* mutants (F). Scale bars: 20 μ m.

embryo were affected (Fig. 6B). This defect became more pronounced when we ectopically expressed *UAS-slit* in the engrailed stripes in *slit* mutant embryos. Fifty-two percent of the dorsal trunk fusion events were disrupted ($n=240$); the dorsal trunk branches, instead of extending anteriorly and posteriorly, seemed to elongate dorsoventrally along the ectopic source of Slit (Fig. 6C). These results suggest that endogenous Slit is required for the migration of the dorsal trunk branches and that ectopic Slit expressed on epidermal stripes can redirect this migration to the site of its expression.

To analyze the role of Slit and its receptors in the formation of the visceral branches, we examined the phenotypes in the visceral branches of embryos expressing *UAS-slit* in the midgut visceral mesoderm and other mesodermal tissues under the control of the *twi-GAL4* driver (Fig. 6D,E). In wild-type embryos, six out of the 10 tracheal metameres send visceral branches towards the gut. The most anterior (T1) and posterior (T10) metameres as well as trunk metameres T3 and T9 do not extend any visceral branches (Manning and Krasnow, 1993) (Fig. 6H). Overexpression of *UAS-slit* in the visceral mesoderm generated new visceral branches from T3 in 11% of the embryos (Fig. 6I), indicating that overexpression of *slit* can attract the migration of tracheal cells to the gut and generate new branches.

We then asked whether Robo2 exclusively mediates the attractant function of Slit. We directed *UAS-slit* expression in the visceral mesoderm under the *twi-GAL4* driver in *robo2*⁸ mutants. We could not detect any new branches growing from trunk segments T2 to T9 in the 25 embryos we examined (Fig. 6F), suggesting that *robo2* is necessary to mediate the tracheal attractant function of Slit in the visceral branches. The analysis of *UAS-slit* overexpression in the visceral mesoderm in *robo* mutant embryos revealed a surprising phenotype. 34% of the embryos had extra visceral branches in the trunk segments. These were either new branches deriving either from T3 and T9 or from bifurcations of the wild-type branches in the rest of the metameres (Fig. 6G,J). As the percentage of new branches induced by Slit is threefold higher in *robo* mutants than in the wild-type, the results suggest that *robo* is an antagonist of Robo2 in the Slit-mediated attraction of the visceral branches.

DISCUSSION

Glial cells provide landmarks for tracheal migration inside the CNS

The morphology of GB1 allows the separation of its tour in the

CNS in two parts. In the first part, starting at the entry point into the CNS, GB1 extends broad filopodial projections and moves its cell body and nucleus ~20 μm towards the ventral longitudinal glia. In the second part, the position of the nucleus remains fixed and the tracheal cell sends a 30 μm long extension that navigates first towards the midline and then turns dorsally through a channel towards the dorsal longitudinal glia. We have previously shown that GB1 contacts different groups of glial cells during its migration through the ventral nerve cord (Englund et al., 1999). The results from genetic ablation of different glial landmarks provided evidence for an instructive role of these substrates in steering GB1 migration and extension. In particular, the GB1 midline crossing phenotype observed after the ablation of midline glia argued for a repulsive signaling mechanism that redirects the cell from its route towards the midline.

Attractive and repulsive functions of Slit

The elegant analysis of axonal guidance at the midline of the fly CNS established the Slit repellent signal as major determinant of axonal pathways (Kidd et al., 1999; Kidd et al., 1998a; Rothberg et al., 1990). A gradient of Slit emanating from the midline prevents axons from crossing the midline through the activation of Robo receptors but it also functions as a long range repellent to position axons in distinct lateral fascicles. This later function is mediated by the expression of different combinations of Robo, Robo2 and Robo3 on axons that take distinct positions along the longitudinal tracts (Rajagopalan et al., 2000a; Simpson et al., 2000b).

Mammalian Slit can also function as a positive regulator of axonal elongation and branching of sensory axons from the rat dorsal root ganglia (Wang et al., 1999) and more recently Slit was found to play an attractive role for muscles during their extension to muscle attachment sites on the *Drosophila* epidermis (Kramer et al., 2001). The molecular mechanism behind the different responses to Slit remains unknown. Repulsion versus attraction could reflect a difference in receptor subunit composition or variations in the cytoplasmic signal transduction machinery of the responsive cells. The complex expression pattern of Slit on several tissues close to the growing tracheal branches together with the tracheal migration defects in *slit* mutants indicate that it plays an important role in epithelial cell guidance. Lack of Slit affects the oriented outgrowth of the dorsal, visceral and ganglionic primary branches, the cells of these branches either stall their migration towards the Slit expressing target or they become misrouted. Overexpression of Slit with a mesodermal GAL4 driver is sufficient to attract new branches towards the gut and overexpression of Slit on epidermal stripes running along the dorsoventral axis of the embryo redirects the anteroposterior migration of the dorsal trunk branches along the new sites of Slit expression. This re-orientation phenotype becomes stronger in *slit* mutants indicating that endogenous *slit* provides a migration cue for these branches. The analysis of loss-of-function and overexpression phenotypes indicates that Slit is a chemoattractant for the outgrowth of several primary tracheal branches towards their targets.

The analysis of GB1 phenotypes in *slit* mutants argues for a repellent function at the midline. In the absence of functional Slit from the CNS midline 37% of the GB1 cells cross the midline barrier and ectopic of *slit* on the longitudinal glia

causes GB1 to stall or turn prematurely when it approaches the longitudinal tracts. Thus, Slit functions as a bi-functional guidance signal in the trachea. The tracheal phenotypes of *slit* in primary and secondary branches are not fully penetrant, emphasizing the importance of other signals in guiding the tracheal branches to their targets. What is the relationship of Slit to the known guidance cues? As Slit is required for the outgrowth of some primary branches, one might have expected that overexpression of Slit in the epidermis by *en-GAL4* would partially rescue the complete absence of tracheal branches in *bnl* mutants. We did not detect any branch outgrowth in *bnl* mutant embryos overexpressing *slit* (data not shown), suggesting that the ability to respond to Slit requires the activity of the Bnl/FGF signaling cascade in the trachea. The most prominent primary branch phenotype of *slit* mutants is the sporadic lack of outgrowth of the dorsal branches. Dpp/TGF β signaling is required for the outgrowth of these branches, suggesting that the localized strong expression of the Robo and Robo2 receptors might be regulated by Dpp signaling. The abundance Robo and Robo2 was, however, unaffected in null mutants for the Dpp co-receptor, Thickveins (Tkv), or in embryos overexpressing a dominant active form of Tkv in the trachea (data not shown), suggesting that Dpp is not likely to regulate the tracheal responses to Slit.

Different functions for Robo and Robo2 in the trachea

In CNS and muscle development Slit function is mediated by the Robo receptors (Brose et al., 1999; Kidd et al., 1999; Kidd et al., 1998b; Kramer et al., 2001; Rajagopalan et al., 2000a; Simpson et al., 2000a). *robo* and *robo2* are expressed in the trachea and the tracheal phenotypes of *robo,robo2* double mutant embryos were very similar to the phenotypes of *slit* mutants, indicating that the tracheal responses to Slit are mediated by Robo and Robo2. Robo and Robo2 receptors can form homo- and heterodimers in vitro (Simpson et al., 2000a) and the differences in their expression patterns suggests that they might mediate different responses to Slit. Indeed, the comparison of the phenotypes between the mutants for either of the two receptors genes revealed some intriguing differences. In *robo* embryos, the GBs erroneously cross the midline, suggesting that *slit* signaling via *robo* mediate repulsion away from the midline. In *robo2* mutants on the other hand, GBs fail to enter the CNS, suggesting that Robo2 may mediate an attractive response to Slit. In addition, the stalls in the migration of the dorsal branches detected in *slit* embryos were only found in *robo2* mutants; no stalling phenotypes were detected in the tracheal branches that did not target the CNS in *robo* mutants. There is also a difference between the phenotypes generated by overexpression of *robo* and *robo2*. Overexpression of Robo in GB1 causes most of the branches to turn away from the midline prematurely. This phenotype is much weaker in embryos overexpressing Robo2, indicating that Robo is a more potent repulsive receptor in the GB. In addition, tracheal overexpression of Robo2 cannot rescue the *robo* mutant GB phenotype, even though tracheal expression of Robo can. This result further indicates that Robo and Robo2 are not identical in their output and they cannot simply substitute for one another.

To further investigate whether different receptor complexes may mediate different responses to Slit, we took advantage of

the phenotypes caused by overexpression of Slit in the gut. In wild-type embryos, ectopic Slit can attract new visceral branches to its site of expression. This attractive function of Slit requires Robo2, as overexpression of Slit with the same driver did not induce branch outgrowth in *robo2* mutants. Robo alone cannot mediate the attractive response to Slit in the visceral branches, instead it appears to function as an antagonist of the attractive signal mediated by Slit and Robo 2 in the visceral branches, because the number of new branches induced by Slit in *robo* mutants is three times higher than the number of branches induced under the same conditions in wild-type embryos.

Taken together these results suggest that there are qualitative differences between the cellular responses to Robo and Robo2 activation and that each receptor plays a unique role in the control of tracheal cell migration. What is the basis for this difference?

Migrating growth cones encounter many guidance cues along their paths and these signals can be either attractive, repulsive or bi-functional. The response to a guidance signal is determined by the intracellular domain of its receptor. Bashaw and Goodman (Bashaw and Goodman, 1999) showed that a chimeric receptor with the ectodomain of Frazzled (the receptor that mediate attractive response to Netrin) and the cytoplasmic domain of Robo (the receptor that mediate repulsive response to Slit) mediate a repulsive response to Netrin. The reciprocal Robo-Frazzled chimeric receptor, however, mediated an attractive response to Slit. Thus, a major determinant of the cellular response to a signal is the specific signal transduction machinery that will be activated upon ligand binding. Robo promotes neuronal repulsion at the midline through its cytoplasmic tail which binds directly to Abl, Ena/Vasp (Bashaw et al., 2000) and srGAPs (Wong et al., 2001). These downstream effectors are then thought to directly modulate actin polymerization and cellular extension during axonal pathfinding.

A second mechanism for axon repulsion derives from the thorough studies of Robo and Netrin signaling in vitro with cultured *Xenopus* neurons. There, the cytoplasmic domain of Robo was found to mediate axonal repulsion partly by directly binding to the cytoplasmic domain of the Netrin receptors and thus silencing the attractive Netrin signal (Stein and Tessier-Lavigne, 2001).

Several recent studies of neuronal guidance cues have revealed that the generation of either attractive or repulsive responses by the same ligand also depends on the type of receptor or receptor complex expressed on the surface of the growth cone. Netrins, for example, mediate attraction via DCC homodimer receptor and repulsion via UNC-5 homodimer receptor and DCC/UNC-5 heterodimer receptor (Colavita and Culotti, 1998; Hong et al., 1999; Keleman and Dickson, 2001; Leonardo et al., 1997). Our results suggest a similar scenario for the interpretation of the Slit signal by tracheal cells. Cells expressing the Robo2 homodimer perceive Slit as an attractant, whereas cells expressing the Robo homodimer or the Robo/Robo2 heterodimer perceive it as a repellent. One possible explanation for the different responses to different receptor complexes is that they may activate different subsets of signal transduction pathways inside the tracheal cells. This is not unlikely, as Robo and Robo2 differ in their cytoplasmic domains. Robo2 lacks two of the cytoplasmic motifs that are

found in the Robo receptors in various species (Rajagopalan et al., 2000a; Simpson et al., 2000a), motifs that are required in Robo for it to regulate midline crossing (Kidd et al., 1998a).

In addition to their function in neuronal guidance, vertebrate Slit homologs and their receptors are also involved in the migration of leukocytes (Wu et al., 2001) and lung development (Xian et al., 2001). The dual function of Slit mediated by different receptor complexes in the trachea may represent a general mechanism for its function also in other systems. The identification of downstream effectors of the different receptor complexes will help to elucidate the molecular mechanism that translates the Slit extracellular signals into attractive or repulsive responses.

We are very grateful to B. Dickson, R. Palmer, C. Goodman, A. Hidalgo, C. Klämbt and G. Technau for generously providing numerous fly stocks and antisera. We thank R. Cantera, M. Mannervik and members of our laboratory for comments on the manuscript. This work was supported by a grant from the Swedish Research Council to C. S.

REFERENCES

- Bashaw, G. J. and Goodman, C. S. (1999). Chimeric axon guidance receptors: the cytoplasmic domains of Slit and Netrin receptors specify attraction versus repulsion. *Cell* **97**, 917-926.
- Bashaw, G. J., Kidd, T., Murray, D., Pawson, T. and Goodman, C. S. (2000). Repulsive axon guidance: Abelson and Enabled play opposing roles downstream of the Roundabout receptor. *Cell* **101**, 703-715.
- Battye, R., Stevens, A. and Jacobs, J. R. (1999). Axon repulsion from the midline of the *Drosophila* CNS requires *slit* function. *Development* **126**, 2475-2481.
- Brand, A. H. and Perrimon, N. (1993). Targeted gene expression as a means of altering cell fates and generating dominant phenotypes. *Development* **118**, 401-415.
- Brose, K., Bland, K. S., Wang, K. H., Arnott, D., Henzel, W., Goodman, C. S., Tessier-Lavigne, M. and Kidd, T. (1999). Slit proteins bind Robo receptors and have an evolutionarily conserved role in repulsive axon guidance. *Cell* **96**, 795-806.
- Campos-Ortega, A. J. and Hartenstein, V. (1985). *The Embryonic Development of Drosophila melanogaster*. New York: Springer-Verlag.
- Colavita, A. and Culotti, J. G. (1998). Suppressors of ectopic UNC-5 growth cone steering identify eight genes involved in axon guidance in *Caenorhabditis elegans*. *Dev. Biol.* **194**, 72-85.
- Englund, C., Uv, A. E., Cantera, R., Mathies, L. D., Krasnow, M. A. and Samakovlis, C. (1999). *adrift*, a novel *bhl*-induced *Drosophila* gene, required for tracheal pathfinding into the CNS. *Development* **126**, 1505-1514.
- Finley, K. D., Edeen, P. T., Foss, M., Gross, E., Ghbeish, N., Palmer, R. H., Taylor, B. J. and McKeown, M. (1998). *dissatisfaction* encodes a Tailless-like nuclear receptor expressed in a subset of CNS neurons controlling *Drosophila* sexual behavior. *Neuron* **21**, 1363-1374.
- Hidalgo, A., Urban, J. and Brand, A. H. (1995). Targeted ablation of glia disrupts axon tract formation in the *Drosophila* CNS. *Development* **121**, 3703-3712.
- Hong, K., Hinck, L., Nishiyama, M., Poo, M., Tessier-Lavigne, M. and Stein, E. (1999). A ligand-gated association between cytoplasmic domains of UNC5 and DCC family receptors converts Netrin-induced growth cone attraction to repulsion. *Cell* **97**, 927-941.
- Hummel, T., Schimmelpfeng, K. and Klämbt, C. (1999). Commissure formation in the embryonic CNS of *Drosophila*. *Dev. Biol.* **209**, 381-398.
- Ito, K., Urban, J. and Technau, G. M. (1995). Distribution, classification and development of *Drosophila* glial cells in the late embryonic and early larval ventral nerv cord. *Roux's Arch. Dev. Biol.* **204**, 284-307.
- Keleman, K. and Dickson, B. J. (2001). Short- and long-range repulsion by the *Drosophila* Unc5 Netrin receptor. *Neuron* **32**, 605-617.
- Kidd, T., Brose, K., Mitchell, K. J., Fetter, R. D., Tessier-Lavigne, M., Goodman, C. S. and Tear, G. (1998a). Roundabout controls axon crossing of the CNS midline and defines a novel subfamily of evolutionarily conserved guidance receptors. *Cell* **92**, 205-215.

- Kidd, T., Russell, C., Goodman, C. S. and Tear, G.** (1998b). Dosage-sensitive and complementary functions of Roundabout and Commissureless control axon crossing of the CNS midline. *Neuron* **20**, 25-33.
- Kidd, T., Bland, K. S. and Goodman, C. S.** (1999). Slit is the midline repellent for the Robo receptor in *Drosophila*. *Cell* **96**, 785-794.
- Kramer, S. G., Kidd, T., Simpson, J. H. and Goodman, C. S.** (2001). Switching repulsion to attraction: Changing responses to Slit during transition in mesoderm migration. *Science* **292**, 737-740.
- Leonardo, E. D., Hinck, L., Masu, M., Keino-Masu, K., Ackerman, S. L. and Tessier-Lavigne, M.** (1997). Vertebrate homologues of *C. elegans* UNC-5 are candidate netrin receptors. *Nature* **386**, 833-838.
- Manning, G. and Krasnow, M. A.** (1993). *Development of the Drosophila tracheal system*. Cold Spring Harbor, New York: Cold Spring Harbor Laboratory Press.
- Moffat, K. G., Gould, J. H., Smith, K. and O'Kane, C. J.** (1992). Inducible cell ablation in *Drosophila* by cold-sensitive ricin A chain. *Development* **114**, 681-687.
- Perrimon, N., Noll, E., McCall, K. and Brand, A.** (1991). Generating lineage-specific markers to study *Drosophila* development. *Dev. Genet.* **12**, 238-252.
- Rajagopalan, S., Nicolas, E., Vivanco, V., Berger, J. and Dickson, B. J.** (2000b). Crossing the midline: roles and regulation of Robo receptors. *Neuron* **28**, 767-777.
- Rajagopalan, S., Vivanco, V., Nicolas, E. and Dickson, B. J.** (2000a). Selecting a longitudinal pathway: Robo receptors specify the lateral position of axons in the *Drosophila* CNS. *Cell* **103**, 1033-1045.
- Rothberg, J. M., Hartley, D. A., Walther, Z. and Artavanis-Tsakonas, S.** (1988). *slit*: An EGF-homologous locus of *D. melanogaster* involved in the development of the embryonic central nervous system. *Cell* **55**, 1047-1059.
- Rothberg, J. M., Jacobs, J. R., Goodman, C. S. and Artavanis-Tsakonas, S.** (1990). *slit*: An extracellular protein necessary for development of midline glia and commissural axon pathways contains both EGF and LRR domains. *Genes Dev.* **4**, 2169-2187.
- Samakovlis, C., Hacohen, N., Manning, G., Sutherland, D., Guillemin, K. and Krasnow, M. A.** (1996a). Development of the *Drosophila* tracheal system occurs by a series of morphologically distinct but genetically coupled branching events. *Development* **122**, 1395-1407.
- Samakovlis, C., Manning, G., Steneberg, P., Hacohen, N., Cantera, R. and Krasnow, M. A.** (1996b). Genetic control of epithelial tube fusion during *Drosophila* tracheal development. *Development* **122**, 3531-3536.
- Seeger, M., Tear, G., Ferres-Marco, D. and Goodman, C. S.** (1993). Mutations affecting growth cone guidance in *Drosophila*: Genes necessary for guidance toward or away from the midline. *Neuron* **10**, 409-426.
- Shiga, Y., Tanaka-Matakatsu, M. and Hayashi, S.** (1996). A nuclear GFP/b-galactosidase fusion protein as a marker for morphogenesis in living *Drosophila*. *Dev. Growth Diff.* **38**, 99-106.
- Simpson, J. H., Kidd, T., Bland, K. S. and Goodman, C. S.** (2000a). Short-range and long-range guidance by Slit and its Robo receptors: Robo and Robo2 play distinct roles in midline guidance. *Neuron* **28**, 753-766.
- Simpson, J. H., Bland, K. S., Fetter, R. D. and Goodman, C. S.** (2000b). Short-range and long-range guidance by Slit and its Robo receptors: A combinatorial code of Robo receptors controls lateral position. *Cell* **103**, 1019-1032.
- Stein, E. and Tessier-Lavigne, M.** (2001). Hierarchical organization of guidance receptors: Silencing of Netrin attraction by Slit through a Robo/DCC receptor complex. *Science* **291**, 1928-1938.
- Sutherland, D., Samakovlis, C. and Krasnow, M. A.** (1996). *branchless* encodes a *Drosophila* FGF homolog that controls tracheal cell migration and the pattern of branching. *Cell* **87**, 1091-1101.
- Tear, G., Harris, R., Sutaria, S., Kilomanski, K., Goodman, C. S. and Seeger, M. A.** (1996). *commissureless* controls growth cone guidance across the CNS midline in *Drosophila* and encodes a novel membrane protein. *Neuron* **16**, 501-514.
- Van Vactor, D., Sink, H., Fambrough, D., Tsoo, R. and Goodman, C. S.** (1993). Genes that control neuromuscular specificity in *Drosophila*. *Cell* **73**, 1137-1153.
- Wang, K. H., Brose, K., Arnott, D., Kidd, T., Goodman, C. S., Henzel, W. and Tessier-Lavigne, M.** (1999). Biochemical purification of a mammalian slit protein as a positive regulator of sensory axon elongation and branching. *Cell* **96**, 771-784.
- Wong, K., Ren, X.-R., Huang, Y.-Z., Xie, Y., Liu, G., Saito, H., Tang, H., Wen, L., Brady-Kalnay, S. M., Mei, L. et al.** (2001). Signal transduction in neuronal migration: Roles of GTPase activating proteins and the small GTPase Cdc42 in the Slit-Robo pathway. *Cell* **107**, 209-221.
- Wu, J. Y., Feng, L., Park, H.-T., Havlioglu, N., Wen, L., Tang, H., Bacon, K. B., Jiang, Z.-H., Zhang, X.-C. and Rao, Y.** (2001). The neuronal repellent Slit inhibits leukocyte chemotaxis induced by chemotactic factors. *Nature* **410**, 948-952.
- Xian, J., Clark, K. J., Fordham, R., Pannell, R., Rabbitts, T. H. and Rabbitts, P. H.** (2001). Inadequate lung development and bronchial hyperplasia in mice with a targeted deletion in the *Dutt1/Robo1* gene. *Proc. Natl. Acad. Sci. USA* **98**, 15062-15066.